

Nondestructive detection of atom counts in laser-trapped ^{171}Yb atoms

Congcong Tian(田聪聪), Qiang Zhu(朱强), Bing Wang(王兵), Dezhi Xiong(熊德智), Zhuanxian Xiong(熊转贤), Lingxiang He(贺凌翔), and Baolong Lyu(吕宝龙)

Citation : Chin. Phys. B, 2025, 34 (**2**): 023201. DOI: 10.1088/1674-1056/ad9e9d
Journal homepage: http://cpb.iphy.ac.cn; http://iopscience.iop.org/cpb

What follows is a list of articles you may be interested in

A miniaturized spin-exchange relaxation-free atomic magnetometer based on uniform light field

Jiajie Li(李佳洁), Xiujie Fang(房秀杰), Renjie Li(李任杰), Baodong Chen(陈宝栋), Yueyang Zhai(翟跃阳), and Ying Liu(刘颖)

Chin. Phys. B, 2023, 32 (**5**): 053201. DOI: 10.1088/1674-1056/aca7f2

Integrated, reliable laser system for an ^{87}Rb cold atom fountain clock

Zhen Zhang(张镇), Jing-Feng Xiang(项静峰), Bin Xu(徐斌), Pan Feng(冯盼), Guang-Wei Sun(孙广伟),Yi-Ming Meng(孟一鸣), Si-Min-Da Deng(邓思敏达), Wei Ren(任伟),Jin-Yin Wan(万金银), and De-Sheng Lü(吕德胜)

Chin. Phys. B, 2023, 32 (**1**): 013202. DOI: 10.1088/1674-1056/ac9e95

Modulation of multiphoton resonant high-order harmonic spectra driven by two frequency-comb fields

Yuanyuan Zhao(赵媛媛), Di Zhao(赵迪), Chen-Wei Jiang(蒋臣威), Fu-li Li(李福利)

Chin. Phys. B, 2018, 27 (**5**): 053202. DOI: 10.1088/1674-1056/27/5/053202

A new fully quantum-mechanical method used to calculate the collisional broadening coefficients and shift coefficients of Rb D_1 lines perturbed by noble gases He and Ar

Wei Zhang(张伟), Yanchao Shi(史彦超), Bitao Hu(胡碧涛), Yi Zhang(张毅)

Chin. Phys. B, 2018, 27 (**1**): 013201. DOI: 10.1088/1674-1056/27/1/013201

Interactions of ion acoustic multi-soliton and rogue wave with Bohm quantum potential in degenerate plasma

M S Alam, M G Hafez, M R Talukder, M Hossain Ali

Chin. Phys. B, 2017, 26 (**9**): 095203. DOI: 10.1088/1674-1056/26/9/095203

Nondestructive detection of atom counts in laser-trapped ^{171}Yb atoms

Congcong Tian(田聪聪)[1,2], Qiang Zhu(朱强)[1,†], Bing Wang(王兵)[1], Dezhi Xiong(熊德智)[1], Zhuanxian Xiong(熊转贤)[1], Lingxiang He(贺凌翔)[1,3,‡], and Baolong Lyu(吕宝龙)[1,3]

[1] *Key Laboratory of Atomic Frequency Standards, Innovation Academy for Precision Measurement Science and Technology, Chinese Academy of Sciences, Wuhan* 430071, *China*
[2] *University of Chinese Academy of Sciences, Beijing* 100049, *China*
[3] *Hefei National Laboratory, Hefei* 230088, *China*

(Received 6 November 2024; revised manuscript received 4 December 2024; accepted manuscript online 13 December 2024)

We present the experimental demonstration of nondestructive detection of ^{171}Yb atoms in a magneto-optical trap (MOT) based on phase shift measurement induced by the atoms on a weak off-resonant laser beam. After loading a green MOT of ^{171}Yb atoms, the phase shift is obtained with a two-color Mach–Zehnder interferometer by means of ±45 MHz detuning with respect to the $^1S_0$–$^1P_1$ transition. We measured a phase shift of about 100 mrad corresponding to an atom count of around 5×10^5. This demonstrates that it is possible to obtain the number of atoms without direct destructive measurement compared with the absorption imaging method. This scheme could be an important approach towards a high-precision lattice clock for clock operation through suppression of the impact of the Dick effect.

Keywords: ytterbium atoms, Mach–Zehnder interferometer, nondestructive detection, phase shift

PACS: 32.80.Qk, 37.10.De, 07.60.Ly, 95.55.Sh

DOI: 10.1088/1674-1056/ad9e9d **CSTR:** 32038.14.CPB.ad9e9d

1. Introduction

The stability and uncertainty of optical clocks have been greatly improved in recent years. Optical lattice clocks based on ytterbium (Yb) at the National Institute of Standards and Technology have reached 3.2×10^{-19}@36 h, while the strontium (Sr) optical lattice clocks at JILA have an instability of 5.8×10^{-19}@3600 s.[1,2] The systematic uncertainties of optical lattice clocks based on ^{87}Sr and ^{171}Yb atoms have now been improved to 8×10^{-19} and 1.4×10^{-18}, respectively.[1,3] With the excellent performance of these lattice clocks, there are many impressive applications in the fields of fundamental physics,[4] geodesy[5,6] and gravitational wave detection.[7]

The frequency stability of an optical lattice clock is an important factor in denoting its performance. Normally, it is described by the Allan deviation. For an averaging time τ it can be written as[8]

$$\sigma_y(\tau)=\frac{\eta}{Q(S/N)}\sqrt{\frac{T_c}{\tau}}, \tag{1}$$

where η is a factor determined by the shape of the resonance, $Q=\nu/\Delta\nu$, is the quality factor of transition line shape and S/N is the signal to noise ratio during the whole clock cycle T_c. From this formula there are three parameters that can be used to improve the frequency stability: increasing Q and S/N or decreasing T_c.

The whole clock cycle T_c comprises the time cycle for preparing the cold atoms, excitation of the clock transition and servo-controlling the clock laser to the clock transition. Normally, cold atom preparation occupies a large part of the whole clock cycle. Here we have to take into account the concept called the Dick effect.[9] This will degrade the clock stability by worsening S/N when the clock laser samples the cold atoms in a discontinuous way (with dead time), and it results from down-converting the clock laser noise into low-frequency noise.[10–12] The Dick noise originates from the noise of the clock laser.[13–15] It can be minimized by increasing the duty cycle of the clock interrogation by using the cold atoms repeatedly through non-destructive detection.[16] In other words, it is necessary to decrease the time cycle of the clock cycle corresponding to the non-interrogation time.

In this paper, we propose to adopt a non-destructive detection scheme based on phase shift measurement induced by the ^{171}Yb cold atoms in a green magneto-optical trap (MOT) without reloading the cold atoms. It is beneficial to shorten the time sequence for preparing the cold atoms so that the dead time of the clock cycle is decreased. The cold Yb atoms are loaded with a laser cooling and trapping technique at 399 nm and 556 nm, and the non-destructive detection scheme is realized with a bicolor Mach–Zehnder interferometer, which was previously used by the group at JILA to give an error signal

†Corresponding author. E-mail: zhuqiang@apm.ac.cn
‡Corresponding author. E-mail: helx@apm.ac.cn

© 2025 Chinese Physical Society and IOP Publishing Ltd. All rights, including for text and data mining, AI training, and similar technologies, are reserved.

for the laser frequency in a chip rubidium atomic clock.[10]

2. Theoretical analysis

The basic principle of the non-destructive detection scheme is to detect the phase shift accumulated by the cold atoms using a near-resonant probe laser beam. For the case of atomic energy levels with lower and upper states denoted by $|J,F,m_F\rangle$ and $|J',F',m_F'\rangle$, respectively, the probe beam with detuning $\Delta_{F,F'}$ from the transition between the two states will experience a phase shift φ:[16]

$$\varphi = \frac{3\lambda^2(2J'+1)}{4\pi S}\sum_{F,m_F,F',m_F'} N(2F'+1)(2F+1) \times \underbrace{\begin{bmatrix} F' & 1 & F \\ m_F' & q & -m_F \end{bmatrix}^2}_{\text{Wigner } 3j \text{ symbol}} \underbrace{\begin{Bmatrix} J & J' & 1 \\ F' & F & I \end{Bmatrix}^2}_{\text{Wigner } 6j \text{ symbol}} \frac{(\Gamma/2)\Delta_{F,F'}}{\Delta_{F,F'}^2+(\Gamma/2)^2}, \quad (2)$$

where N is the atomic population in the hyperfine substate $|J,F,m_F\rangle$, q is the polarization state, λ is the wavelength of the probe beam, $\Delta_{F,F'}$ is the laser detuning to the resonance, Γ is the natural linewidth of the transition and S is the cross section of the atomic cloud. For a laser beam with Gaussian distribution, the cross section $S = 2\pi(r_0^2 + w^2/4)$, where r_0 is the atomic cloud standard deviation and w is the $1/e^2$ radius of the laser beam.

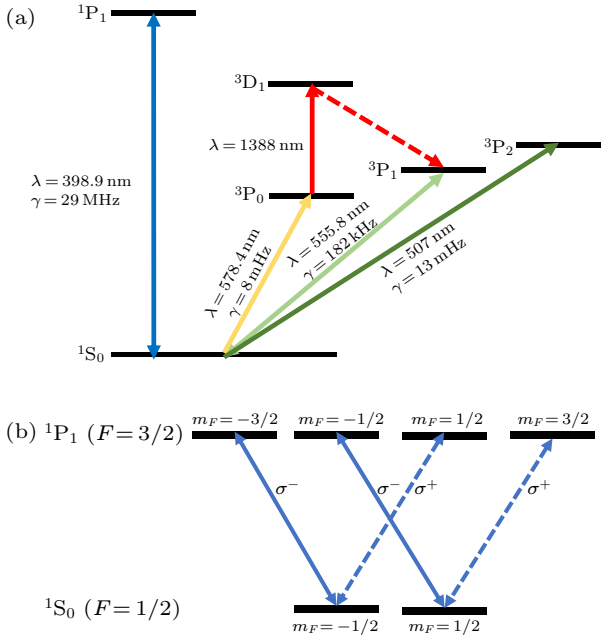


Fig. 1. The main energy levels involved in the non-destructive probing scheme for ^{171}Yb. (a) The main energy level structure of ^{171}Yb. (b) The ^{1}S$_0$ ($F=1/2$)→^{1}P$_1$ ($F'=3/2$) transition involved in the non-destructive probing scheme.

When we consider the non-destructive detection scheme for Yb atoms, the probe beam is in resonance with the ^{1}S$_0$ ($F=1/2$)→^{1}P$_1$ ($F'=3/2$) transition, so $F=1/2$, $F'=3/2$, $m_F=1/2$, $m_F'=3/2$, $J=0$, $J'=1$, $q=-1$ and $I=1/2$; the related energy levels of the Yb atoms are depicted in Fig. 1 from the results of Stone's Wigner coefficient calculator,[17] We can get

$$\begin{pmatrix} 3/2 & 1 & 1/2 \\ 3/2 & -1 & -1/2 \end{pmatrix} = -1/2, \quad \begin{Bmatrix} 0 & 1 & 1 \\ 3/2 & 1/2 & 1/2 \end{Bmatrix} = -\sqrt{1/6},$$

so Eq. (2) is changed to

$$\varphi_{\text{atom}} = \frac{3\lambda^2 N}{4\pi S} \times 3 \times 4 \times 2 \times (1/4) \times (1/6) \times \frac{(\Gamma/2)\Delta_{F,F'}}{\Delta_{F,F'}^2+(\Gamma/2)^2} = \frac{3\lambda^2 N}{4\pi S} \times \left(\frac{(\Gamma/2)\Delta_{F,F'}}{\Delta_{F,F'}^2+(\Gamma/2)^2}\right). \quad (3)$$

Figure 2 shows that φ_{atom} has a simple relationship with atom counts N staying in the MOT. That is to say, once one extracts the phase shift, the atomic population of the cold atomic cloud can be easily obtained. For a 45 MHz detuning, the phase shift is about 50 mrad, which corresponds to an atomic number about $N = 5\times10^5$ with $S = 1.12\times10^5$ μm^2.

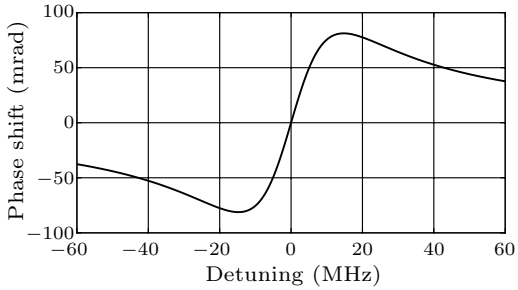


Fig. 2. Theoretical calculation of the phase shift along with the detuning for the Yb ^{1}S$_0$–^{1}P$_1$ transition probe.

3. Experimental setup

Based on the above theoretical analysis, we built the cold atomic experimental setup shown in Fig. 3. The apparatus mainly consists of an internally heated atomic oven, a cube, an inline valve (MDC Company, MIV-150-V), a mechanical baffle, a differential tube and a science chamber. The line valve divides the whole system into the oven area on the left and the science chamber area on the right, and two ion pumps are equipped on each side to maintain a high vacuum level. A thin differential tube connects the oven side and science chamber side to ensure a vacuum difference of about two orders of magnitude. A cube behind the oven is used for transverse cooling to reduce the beam divergence angle. A mechanical baffle blocks the beam flow when the system is not in operation. The chamber has eight 2.75-in windows in the horizontal plane, with three pairs of six optical channels in the horizontal plane in addition to the left channel used for the atomic beam and the right channel used for Zeeman beam. In the vertical plane, there are two 4.5-in viewing windows, and two anti-Helmholtz coils are mounted on the outside of these two windows to generate the quadrupole MOT magnetic field (not shown in the figure), with cooling water channels inside to remove the heat from the coils.

The Yb atomic oven is baked to 350 °C and the velocity of the hot atomic beam follows the Maxwell–Boltzmann distribution. In order to load the blue MOT efficiently, the atomic beam has to be pre-cooled with a Zeeman slower. Our Zeeman beam is designed with a laser power about 15 mW at 399 nm (detuned–300 MHz) without Zeeman coils. The 399 nm laser was developed with injection-locking technology (Moglabs Company, ILA). A MOT is formed with six beams of about 8 mW (detuned–28 MHz) and a pair of anti-Helmholtz coils (magnetic field gradient about 40 G·cm^{-1}). After the blue MOT has been loaded with the 399 nm laser, the 556 nm laser (Precilasers, YFL-SSHG-556-0.2-CW) is used to load the cold atoms into the green MOT. For the green MOT, each beam is about 1.5 mW, with detuning of 200 kHz, and the magnetic field gradient is dropped to 12 G·cm^{-1}. The probe light is about 2 mW, which is off-resonance with the $^1S_0 \rightarrow {}^1P_1$ transition, with detuning of about ±45 MHz.

The time sequence for non-destructive detection is shown in Fig. 4. The Zeeman and first-stage cooling beam are switched on for 1.5 s to collect the maximum atom count in the blue MOT. The 556 nm beam for the second-stage cooling and the probe beam at 399 nm for non-destructive detection are kept on for 2 s. The duration of the green MOT is 0.5 s.

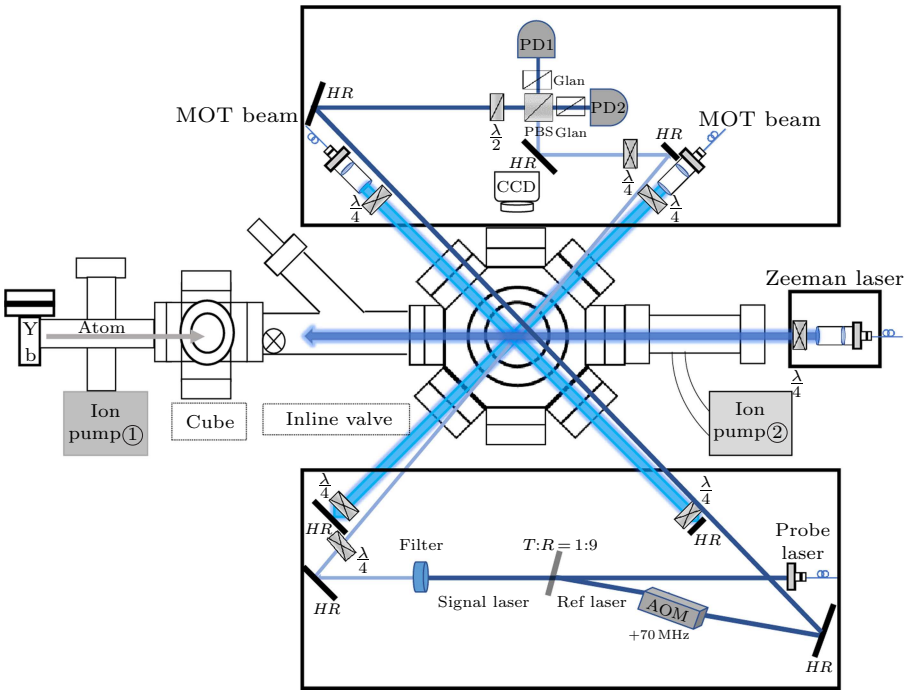


Fig. 3. Schematic diagram of the vacuum system and the laser path for the nondestructive measurement.

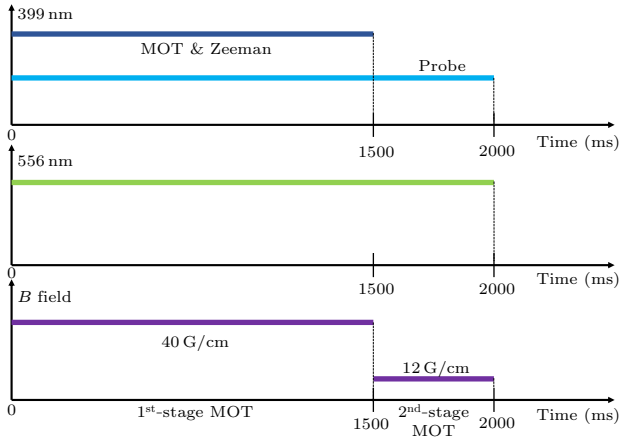


Fig. 4. Time sequence for non-destructive detection including the Zeeman beam, two-stage MOT beams and the magnetic field.

After the green MOT has been loaded, another 399 nm laser beam is used as the probe to build a two-color Mach–Zehnder interferometer for the nondestructive detection scheme, as shown in Fig. 5. The probe laser is separated into two beams with P^- and P^+ components, where one beam is red-detuned and the other is blue-detuned with the same value at 45 MHz. A beamsplitter (T:R = 1 : 9) is used to separate the probe beam into a reference beam and a signal beam, with the stronger reflected beam as the reference beam and the weaker transmitted one as the signal beam. The reference beam passes through an acousto-optic modulator (AOM) modulated at 70 MHz, and then goes through the science chamber bypassing the atomic cloud. The signal beam passes through a neutral density filter to reduce the light intensity to the 100 nW level, and is then focused on the cold atoms. A polarizing beam splitter is used to combine the reference and the signal into the same channel; the polarizations of the two channels are perpendicular to each other. Before the photodetectors (PDs), two 45° Glan–Taylor prisms are also arranged to obtain the beating signal.

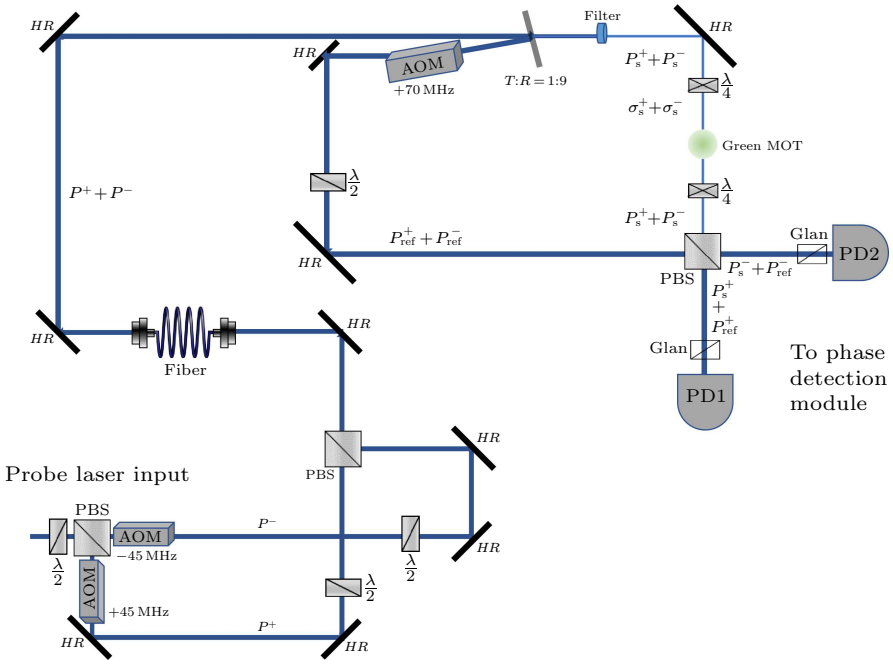


Fig. 5. The experimental scheme for measuring the phase shift of cold atoms using a two-color Mach–Zehnder interferometer (AOM, acousto-optic modulator; PBS, polarizing beam splitter; PD, photodetector).

We first record the image of the atomic cloud in the green MOT with a charge-coupled device camera and measure the size of the atomic cloud, with its radius of about 120 μm. Then, we select a lens assembly to match the probe laser beam size with the atomic cloud. We measure the beam waist with an analyzer (Dataray Company, WinCamD-1310) at the focus. The laser waist radius is about 125 μm. The first $\lambda/4$ wave-plate on the signal side changes the signal light into left-hand and right-hand circularly polarized light. When the signal light passes through the cold atoms, the σ^+ and σ^- transitions of the atoms will be excited and a phase shift generated.

The outputs from the bicolor Mach–Zehnder interferometer are recorded by two photodetectors (PD1 and PD2), and the outputs of the two PDs can be written as follows:[10]

$$s_1 \propto \sqrt{P_s^+ P_{ref}^+}\cos(\omega_m t + \Delta\varphi^+ + \varphi_1), \tag{4}$$

$$s_2 \propto \sqrt{P_s^- P_{ref}^-}\cos(\omega_m t + \Delta\varphi^- + \varphi_2). \tag{5}$$

Here P_s^+ and P_s^- are the signal light intensities, P_{ref}^+ and P_{ref}^- are the reference light intensities, ω_m is the modulation frequency of the AOM, $\Delta\varphi^+$ and $\Delta\varphi^-$ are the phase shifts caused by the atoms, and their relation is $\Delta\varphi^+ = -\Delta\varphi^- = \varphi_{atom}$. φ_1 and φ_2 are the phase shifts originated from the length difference between the interferometer arms. In our two-color interferometer configuration, $\varphi_1 = \varphi_2$.

The signals from the PDs first pass through a bandpass filter (Mini-Circuits Company, SXBP-69+) with a center frequency of 69 MHz, which is used to filter out other frequency components except the 70 MHz signal (mainly the frequency component around 90 MHz). The bandpass filter provides −30 dB attenuation, which effectively removes these interference components. Two limiting amplifiers are used to amplify the signal, which is then fed into a phase detector (Mini-Circuits Company, RPD-1+) for phase detection. Finally, the output is set to a low-pass filter and amplified again to the oscilloscope, as shown in Fig. 6.

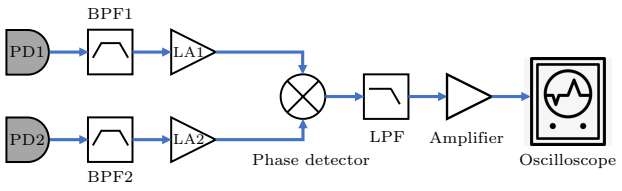


Fig. 6. The block diagram of phase shift detection (BPF, bandpass filter; LA, limiting amplifier; LPF, low-pass filter; PD, photodetector).

The final output signal of the phase detection circuit can be written in the following form:

$$\text{Signal} = A\sin(\varphi_m + 2\varphi_{atom}). \tag{6}$$

Here A is the signal amplitude and φ_m is an electric phase shift caused by different signal delays during the transmission of two beating signals. In the ideal case it stays constant and does not change with time. φ_{atom} is the atomic phase shift signal to be measured. By phase compensation and eliminating φ_m in Eq. (6), the relationship between the measured signal amplitude and the phase shift can be approximately simplified to $\text{Signal} = 2A\varphi_{atom}$. To obtain the coefficient A, two 70 MHz signals are generated using a commercial signal source and fed together into the two inputs of the detection circuit. By varying their phase difference, we obtain the relationship between the phase difference and the size of the output signals. From

the fitting result, we obtain the sensitivity $A = 0.63\ \mathrm{V{\cdot}rad^{-1}}$ as shown in Fig. 7.

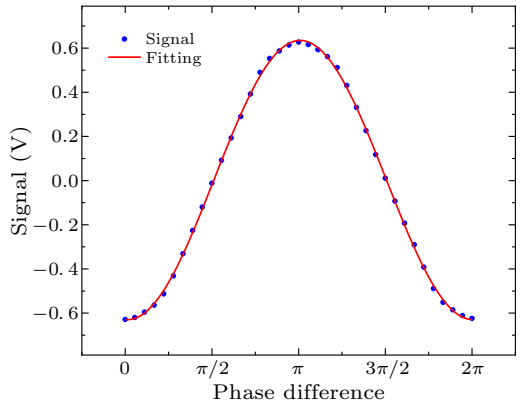


Fig. 7. Measurement of the phase difference sensitivity. The blue points are the measured values and the red line is the fitting curve based on Eq. (6).

4. Results and discussion

The phase shift is obtained from the output of the phase difference detection circuit, and is shown in Fig. 8. It can be easily seen that the signal given by the phase difference detection circuit is a step signal when the cold atoms are loaded into the green MOT, and then reverts to the initial value at the end of the green MOT stage. During the green MOT loading stage, a clear step signal appears above the bottom level. The height of this step is about 40–80 mV, and the phase shift φ_{atom}, and the phase shift due to the green MOT atoms is calculated to be around 30–60 mrad according to Eq. (6), which approximates 50 mrad predicted by the theory in Fig. 2. With the experimentally measured parameters brought into Eq. (3), we can obtain an atom count of about (3–6) $\times$ 10^5. Our result is also in agreement with the phase shift measurements performed by the LNE-SYRTE group on Sr atoms.[16]

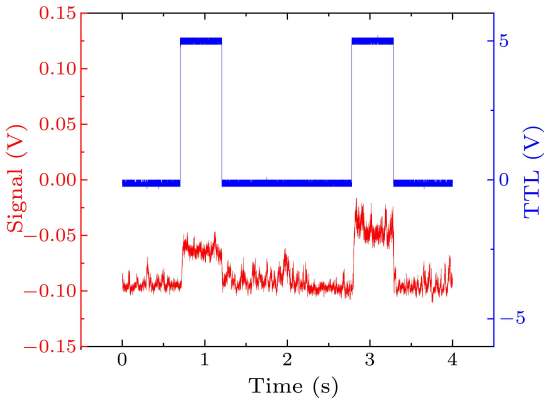


Fig. 8. Recorded phase shift signals from non-destructive detection in a green MOT. The blue TTL signal (right y-axis) indicates the state of the green MOT, with cold atoms (high level) and without atoms (low level). The red line (left y-axis) is the phase shift signal from the phase difference detection circuit.

The fact that there are large fluctuations in our phase shift measurement could be due to several reasons. Firstly, imperfect frequency locking at 556 nm with a reference cavity makes the optimal frequency jitter from time to time around a natural linewidth. Secondly, the power of the trapping laser fluctuates because of imperfect polarization matching with the fiber axis. These two factors will partially contribute to the detection noise.

5. Conclusion

In summary, we have experimentally demonstrated a non-destructive measurement scheme in cold Yb atoms based on a bicolor Mach–Zehnder interferometer. With this interferometer we have successfully obtained atom counts of around 5×10^4 from the phase shift caused by the cold atoms. This indicates that it is feasible to approximately estimate the atom counts by this method instead of imaging method. This non-destructive detection method can be used in our Yb optical clocks,[18–20] which will suppress the Dick effect and improve the frequency stability of Yb clocks in the future.

Data availability statement

The data that support the findings of this study are openly available in Anthony Stone's Wigner coefficient calculator website at https://www-stone.ch.cam.ac.uk/wigner.shtml.

Acknowledgements

Project supported by the National Natural Science Foundation of China (Grant Nos. U20A2075, 11803072, and 12374467), the Innovation Program for Quantum Science and Technology (Grant No. 2021ZD0300902), and the Hubei Provincial Science and Technology Major Project (Grant No. ZDZX2022000004).

References

[1] McGrew W F, Zhang X, Fasano R J, Schäffer S A, Beloy K, Nicolodi D, Brown R C, Hinkley N, Milani G, Schioppo M, Yoon T H and Ludlow A D 2018 *Nature* **564** 87
[2] Oelker E, Hutson R B, Kennedy C J, Sonderhouse L, Bothwell T, Goban A, Kedar D, Sanner C, Robinson J M, Marti G E, Matei D G, Legero T, Giunta M, Holzwarth R, Riehle F, Sterr U and Ye J 2019 *Nat. Photonics* **13** 714
[3] Aeppli A, Kim K, Warfield W, Safronova M S and Ye J 2024 *Phys. Rev. Lett.* **133** 023401
[4] Safronova M S, Budker D, DeMille D, Kimball D F J, Derevianko A and Clark C W 2018 *Rev. Mod. Phys.* **90** 025008
[5] Grotti J, Koller S, Vogt S, *et al.* 2018 *Nat. Phys.* **14** 437
[6] Mehlstäubler T E, Grosche G, Lisdat C, Schmidt P O and Denker H 2018 *Rep. Prog. Phys.* **81** 064401
[7] Kolkowitz S, Pikovski I, Langellier N, Lukin M D, Walsworth R L and Ye J 2016 *Phys. Rev. D* **94** 124043
[8] Quessada A, Kovacich R P, Courtillot I, Clairon A, Santarelli G and Lemonde P 2003 *J. Opt. B: Quantum Semiclass. Opt.* **5** S150
[9] Prestage J D, Dick G J and Maleki L 1989 *J. Appl. Phys.* **66** 1013
[10] Farkas D M, Zozulya A and Anderson D Z 2010 *Appl. Phys. B* **101** 705
[11] ten Brinke N and Schützhold R 2016 *Eur. Phys. J. D* **70** 102
[12] Westergaard P G, Lodewyck J and Lemonde P 2010 *IEEE Trans. Ultrason. Ferroelectr. Freq. Control* **57** 623
[13] Zhang W, Robinson J M, Sonderhouse L, Oelker E, Benko C, Hall J L, Legero T, Matei D G, Riehle F, Sterr U and Ye J 2017 *Phys. Rev. Lett.* **119** 243601

[14] Matei D G, Legero T, Grebing C, Häfner S, Lisdat C, Weyrich R, Zhang W, Sonderhouse L, Robinson J M, Riehle F, Ye J and Sterr U 2016 *8th Symposium on Frequency Standards and Metrology* Oct. 12-16 2015 Potsdam, Germany

[15] Keller J, Ignatovich S, Webster S A and Mehlstäubler T E 2014 *Appl. Phys. B* **116** 203

[16] Lodewyck J, Westergaard P G and Lemonde P 2009 *Phys. Rev. A* **79** 061401

[17] Klink W H and Wickramasekara S 2010 *Eur. J. Phys.* **31** 1021

[18] Zhang A, Xiong Z A X, Chen X T, Jiang Y Y, Wang J Q, Tian C C, Zhu Q, Wang B, Xiong D Z, He L X, Ma L S and Lyu B L 2022 *Metrologia* **59** 065009

[19] Wang J Q, Zhang A, Tian C C, Yin N, Zhu Q, Wang B, Xiong Z X, He L X and Lv B L 2022 *Chin. Phys. B* **31** 090601

[20] Liu H, Zhang X, Jiang K L, Wang J Q, Zhu Q, Xiong Z X, He L X and Lyu B L 2017 *Chin. Phys. Lett.* **34** 020601